Excitation Transfer in the Core Light-Harvesting Complex (LH-1) of *Rhodobacter sphaeroides*: An Ultrafast Fluorescence Depolarization and Annihilation Study

Stephen E. Bradforth,[†] Ralph Jimenez,[†] Frank van Mourik,[‡] Rienk van Grondelle,*[,‡] and Graham R. Fleming*[,†]

Department of Chemistry and James Franck Institute, University of Chicago, Chicago, Illinois 60637, and Department of Physics and Astronomy, Free University of Amsterdam, de Boelelaan 1081, 1081 HV Amsterdam, The Netherlands

Received: May 31, 1995; In Final Form: August 15, 1995[⊗]

The depolarization of the bacteriochlorophyll fluorescence from the core light-harvesting antenna (LH-1) of *Rhodobacter sphaeroides* was time-resolved using fluorescence upconversion. Complexes isolated in the detergent octylglucoside and chromatophores of the LH-1-only mutant M2192 were studied. For both preparations, the anisotropy of the fluorescence drops from an initial value of ~0.4 to 0.07 with a biphasic decay characterized by time constants of approximately 110 and 400 fs. The decay of the anisotropy is modeled as energy transfer between bacteriochlorophyll dimers in the antenna. The results are discussed in relation with current models for the structural organization of the core antenna. Numerical modeling of the observed annihilation processes indicates a domain size of approximately 16 pigments (eight dimers) for detergent-isolated LH-1 complexes. Simulations show that the depolarization data are consistent with either a symmetric ring structure and an inhomogeneous spectral distribution function for the pigments or a ring made up of pigment clusters. Oscillations in the isotropic fluorescence with a 105 cm^{-1} frequency suggest wave-packet motion in the excited state chromophore in analogy with the reaction center special pair, for which a similar frequency is observed in time domain experiments. These oscillations are supporting evidence for the hypothesis that the LH-1 antenna is built of bacteriochlorophyll dimers. The dephasing of the oscillations is slower than the observed depolarization time scale.

Introduction

The primary processes in photosynthesis have been the subject of a large number of time-resolved spectroscopic studies. In particular, the photosynthetic purple bacteria are suitable for the study of biological energy- and electron-transfer processes[1] since their photosynthetic apparatus is significantly less complex than that of algae and higher plants. Moreover, for two purple bacterial species, *Rhodobacter (Rb.) sphaeroides* and *Rhodopseudomonas (Rps.) viridis*, the structure of the photosynthetic reaction center (RC) has been determined by X-ray diffraction of crystals.[2–4] The core light-harvesting antenna (LH-1) of the photosynthetic purple bacteria is the simplest photosynthetic light-harvesting antenna system. X-ray structural data are just becoming available for these bacterial membrane bound antenna complexes,[5] although no high-resolution structure is available yet for LH-1. The available structural evidence suggests that these antennae form highly symmetric ring structures and that energy is stored by extremely rapid energy migration within the ring.

The challenge is now to understand how the excitation-transfer dynamics takes place within these complexes and how nature has designed a molecular architecture which achieves such high overall efficiency in harvesting sunlight. This means exploring fully the relationship between the structural arrangement of pigments and the mechanisms of energy transport under physiological conditions. Various time- and frequency-resolved spectroscopies allow us to observe directly energy migration time scales, investigate the nature of pigment–pigment couplings, and study the effects of structural and energetic disorder and the coupling to the environment on the appropriate physical description of this electronic energy migration. In this study we observe this excitation migration within the LH-1 antenna via ultrafast depolarization of fluorescence and by time-resolved excitation annihilation measurements. The rapidly growing amount of protein structure information for photosynthetic antennae helps enormously in making quantitative models to interpret the results of these dynamical studies.

Models for the molecular organization of the core light-harvesting antenna have been proposed on the basis of numerous biochemical,[6–8,10] spectroscopic,[11–14] and structural studies.[7,9,15–17] The LH-1 antenna is built up from two small polypeptides, α and β, each of which binds one bacteriochlorophyll *a* (BChl *a*). In the intact antenna, the lowest electronic transition of BChl *a* (known as the Q_y band) peaks at 875 nm. With the detergent octylglucoside LH-1 can be reversibly dissociated into a minimal form, B820,[18–20] which has the spectroscopic properties of a strongly coupled dimer of BChl *a*.[14,21] Despite the fact that the absorption maximum of the B820 subunit is blue shifted by about 55 nm relative to the *in vivo* complex, the triplet–singlet (T–S)[14,22] and excited state difference[23] spectra of B820 and LH-1 are very similar. This is a strong indication that the dimeric nature of B820 is maintained in the fully assembled LH-1. Radiation inactivation experiments support this notion: analysis of both the absorption spectrum of LH-1[12] and the EPR signal of oxidized LH-1[13] under these conditions indicates a single $\alpha\beta BChl_2$ basic unit. Throughout this paper we will assume that the pigments of LH-1 can best be described as an assembly of BChl dimers. Rapid-mixing experiments have demonstrated that the association of two B820 complexes is enough to cause most of the absorption red-shift between B820 and LH-1.[24] This would seem to provide evidence that the spectroscopic minimal unit contains four pigments. Whether

* Corresponding authors.
† University of Chicago.
‡ Free University, Amsterdam.
⊗ Abstract published in *Advance ACS Abstracts*, October 1, 1995.

0022-3654/95/2099-16179$09.00/0

this tetramer should be looked upon as one super molecule or as two dimers and whether even larger degrees of delocalization are important for the description of energy migration in the antenna[25,26] are open questions that will be considered in the discussion.

There appears to be some variability reported in the total number of pigments in a given bacterial antenna ring. This variation is most likely between different preparation methods and different bacterial strains rather than an *in vivo* distribution. The structure of the B800-850 complex of *Rhodopseudomonas acidophila* consists of rings of 18 B850 pigments with overall 9-fold symmetry.[5] It is generally agreed that, *in vivo*, LH-1 rings must be larger in diameter (with more pigments) to accommodate the reaction center. The LH-1 antenna from *Rps. viridis* forms a ringlike structure with 6-fold symmetry that surrounds the RC;[15] Stark *et al.* suggest that this corresponds to 24 BChl pigments in the ring. Two-dimensional crystals obtained by reassociating the fully dissociated LH-1 antenna (B820) of *Rhodopseudomonas marina* and *Rhodospirillum rubrum* gave rise to rings with 6-[9] and 16-fold[17] symmetry, containing 24 and 32 BChl pigments per ring, respectively. In the latter study, Karrasch *et al.*[17] also report smaller rings. However, Meckenstock *et al.* suggest that molecular weight evidence points toward subunits of two $\alpha\beta BChl_2$,[8,9] and it is these that make up the constituent elements that are seen with 6-fold symmetry in their 26 Å map. In contrast, Karrasch *et al.*'s 8.5 Å projection map shows no such subunit clustering;[17] rather these authors suggest that the dimers are symmetrically arranged in a ring. Compared to membrane-bound or reassociated LH-1, isolated detergent-solubilized LH-1 complexes tend to be significantly smaller, as observed in electron microscopy.[16,27] The detergent-isolated LH-1 complex was estimated to contain approximately 12 pigments.[16] Note that even with the bound detergent these complexes appear to be significantly smaller in diameter (8−9 nm)[16,27] than the rings observed in the reassociated complexes (11.6 nm).[17] We have therefore included in our study two preparations of LH-1 antennae: an LH-1-only mutant (no reaction center) M2192,[28] whose antennae are present in the native membrane, and detergent-isolated LH-1 complexes.

Energy-transfer processes within the bacterial light-harvesting antenna have been studied using low-intensity picosecond pump−probe[29−34] and fluorescence[35−37] techniques. In these studies the time resolution of the experiment was limited to a few picoseconds. The pump−probe measurements showed no time dependence in the anisotropy of the signals,[29−33] and the initial anisotropy was low ($r(0) < 0.1$) and close to the steady state value,[11] indicating that energy-transfer processes had already occurred on a sub-picosecond time scale. The hopping times derived from singlet−singlet annihilation experiments (0.5−1 ps)[38−40] are certainly consistent with this. Therefore, to study the equilibration/migration processes in the antenna directly, sub-picosecond time resolution is mandatory.

Although the core antenna consists of only one spectral form (B875), inhomogeneous broadening of the spectrum enables the observation of excitation energy transfer between pigments with different site energies in the inhomogeneous distribution. The migration may be observed as the excited state distribution produced by the spectral selection of the excitation pulse changes into a thermal distribution, *i.e.* spectral equilibration. Determination of the extent of inhomogeneous broadening in bacterial antennae has been most successfully made at low temperature by hole-burning spectroscopies.[41] These and other low-temperature spectroscopic studies are in agreement that the absorption spectra of the B820 subunit is predominantly (~300 cm^{-1}) inhomogeneously broadened.[42,43] Hole burning on whole LH-1 membranes indicates only 80 cm^{-1} inhomogeneity at low temperature,[25] whereas low-temperature fluorescence measurements on detergent complexes of LH-1 suggest predominant inhomogeneous broadening.[44] Likewise, low-temperature picosecond measurements for *Rs. rubrum* LH-1 have been simulated with an inhomogeneous model for the antenna.[45,46] An analysis of the temperature dependence of the absorption and emission properties of the B820 subunit of LH-1 suggests that even at room temperature inhomogeneous broadening might prevail.[43,47] Leupold *et al.* indicate that the B850 band in LH-2 (analogous to LH-1's B875) is mainly inhomogeneously broadened at room temperature.[48] Since this corresponds with an inhomogeneous bandwidth of the antenna comparable to k_BT, the equilibration should cause large changes in the time-resolved absorption and emission spectra. Sub-picosecond pump−probe measurements on the LH-1 antenna have indeed demonstrated fast spectral evolution, reflecting the equilibration process both at room temperature[23,26] and at 4 K.[49] The later pump−probe study of LH-1 complexes by Sundström and co-workers, which has attained the best resolution to date (~40 fs), suggests that energy transfer takes place on a ~100 fs time scale.[49,50] The precise interpretation of the observed effects in terms of hopping processes depends on the model used for the structure and spectroscopy of the antenna. The most important factors involved are the connectivity of the antenna (*i.e.* the number of neighboring sites to which an excited pigment/dimer can transfer its energy), the homogeneous linewidth of the chromophores, and the distribution of site energies.

In this work we have studied the energy-transfer process in the LH-1 antenna by measuring the rate of fluorescence depolarization, using the fluorescence upconversion technique. These measurements have a time resolution of ~50 fs. Depolarization is a rather more specific probe of energy-transfer dynamics than time-resolved spectral evolution. For example, energy randomization between identical chromophores in a plane will be manifested by a fluorescence anisotropy decay from $r = 0.4$ to $r = 0.1$; the depolarization time scale is related to the rate of energy transfer. Furthermore, this work also represents the first instance in which sub-picosecond singlet−singlet annihilation measurements have been combined with time-resolved polarized fluorescence to yield information about the energy-transfer hopping time and domain size. In Sundström and co-workers' experiment, strong oscillations in the transient absorption signal were observed.[50] Likewise, in our experiments the isotropic fluorescence contains oscillations with the same dominant beat frequency. Moreover, these beats are similar in frequency to, but much stronger at room temperature than, those observed for the special pair of the bacterial reaction center.[51,52] It should be emphasized that since we monitor only the spontaneous emission, interpretation of the data is simpler in comparison with transient absorption experiments,[50] in which ground state bleaching, excited state absorption, and stimulated emission may all contribute to the signals. This enables assignment of oscillations, if vibrational in origin, to the excited state surface and considerable simplification in understanding the anisotropy of polarized measurements.

Materials and Methods

Two preparations of LH-1 antennae were studied. Membranes of the mutant strain M2192 (which is free of reaction centers and peripheral antennae) of *Rb. sphaeroides* were prepared as described in ref 28. Experiments were performed on a sample in 50 mM phosphate buffer, pH 7.8, with an OD875 of 0.5/mm. In addition, detergent-solubilized LH-1 complexes

isolated from *Rb. sphaeroides* strain PUC 705 BA in the detergent *N*-octyl-β-D-glucopyranoside (BOG, 0.8%) were used. This preparation is also free of other photosynthetic proteins and had an OD875 of ~1.2/mm. Both preparations contain carotenoids. Absorption spectra were taken before and after data collection, and no degradation of either sample was observed.

Fluorescence upconversion measurements were performed using two different laser sources based on a mode-locked Ti: sapphire. Most measurements were made with an oscillator (repetition rate 76 MHz) operating at wavelengths between 850 and 870 nm. For the experiments presented here the bandwidth of the pulses was 10 nm fwhm and the pulsewidth was ca. 110 fs, as determined from the measured autocorrelation assuming a Gaussian pulse form. The amplified laser source used for the annihilation measurements was a 250 kHz regenerative amplifier (Coherent RegA 9000) operating at 870 nm. The width of the amplified pulses was approximately 200 fs. The reflective fluorescence upconversion setup has been described in detail previously.[53] The cell containing the sample is placed at one focus of an elliptical mirror, and a 0.5 mm BBO crystal (type I) is placed at the other focus. A 10 nm bandwidth of fluorescence is upconverted by mixing the laser wavelength with the fluorescence in a noncollinear geometry and tuning the crystal angle. The upconverted fluorescence is collimated with a lens, passed through a 10 nm bandpass filter to improve rejection of one- and two-beam signals at the laser second-harmonic frequency, and then directed into a 0.22 m double monochromator. The signal is detected by a PMT and accumulated with a photon counter for 1 s at each delay position. By variably delaying the gate pulse with respect to the excitation pulse, the fluorescence intensity is measured as a function of time. The step size used for the experiment corresponds to a 6.67 fs delay. Two arrangements were used to flow the sample. Sufficient chromatophore preparation was available to continuously flow this sample in a closed loop, whereas the detergent preparation was held in a quartz static cell and continuously stirred by a platinum wire connected to an electric toothbrush. Both the static and flowing cells had optical path lengths of 1 mm.

The instrument response function (IRF) was measured by tuning the crystal to mix the gate beam with the excitation beam. The IRF is well fit by a Gaussian with a width of ~160 fs fwhm. Both excitation and gate beams passed through 1 cm calcite polarizers, and the polarization of the excitation beam was changed by rotating a zero-order waveplate placed after the polarizer. To verify that accurate polarization measurements can be made in the upconversion apparatus, the fluorescence anisotropy of the dye IR 132 was measured and found to be 0.39 ± 0.02. It was noted however that great care must be taken to avoid saturation to achieve high values for the initial anisotropy. Experiments at 870 nm with shorter (~70 fs) pulses were also performed; however, it became necessary to use an 890 nm cutoff filter (Oriel 58899) to remove the long-wavelength tail in the laser pulse spectrum to avoid contamination of the fluorescence signals around time zero with (upconverted) pump light. The early time anisotropy is extremely sensitive to this effect, and it was found that markedly improved results (with much higher signal-to-noise) arose using the smaller bandwidth laser pulses.

Results

Figure 1 shows the isotropic decay of the LH-1 fluorescence from the detergent-isolated preparation. The complex is excited at 860 nm, and the detected fluorescence is centered at 952 nm.

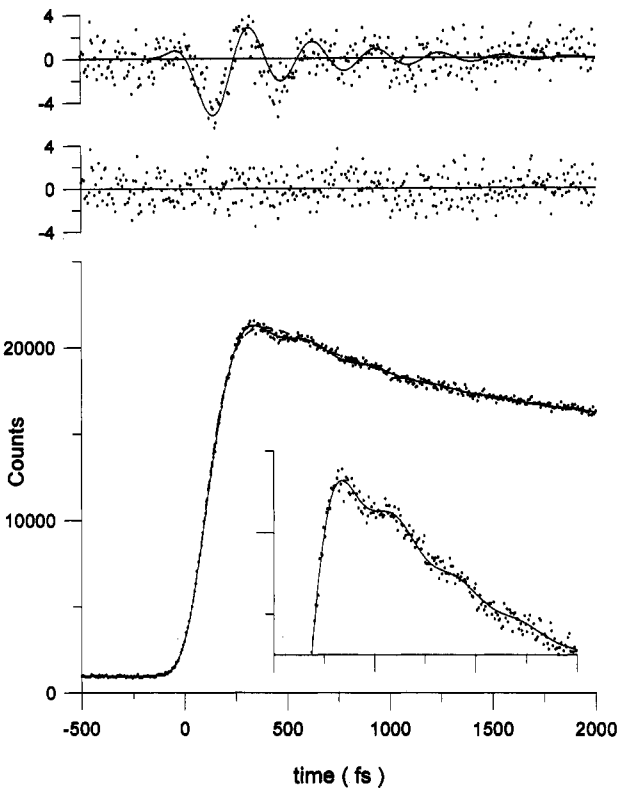

Figure 1. Time-resolved isotropic fluorescence from detergent-isolated LH-1 complexes excited at 860 nm and detected at 952 nm (dots) and fits (without cosine term, dashed; with cosine term, solid). Inset shows oscillations in more detail. (Top) Residuals to fit: upper panel shows residual to fit without cosinusoidal function and a line showing the cosine term that is added into the second fit form; the lower panel shows the residuals to full fit including cosine function.

The decay of the isotropic fluorescence has been measured, with variable excitation energies, over three scan ranges (up to 100 ps) and shows that the lifetime not only is intensity dependent but has three distinct decay components. The ratio of these components changes as a function of the pulse energy and repetition rate. As discussed below, we ascribe the two faster decay time constants to singlet−singlet (S−S) and singlet−triplet (S−T) annihilation.[38−40,54−56] In addition, the short time range scan shows (i) a rise time of ~90 fs and (ii) marked oscillations in the fluorescence intensity. Fitting all three scan ranges self-consistently yields the exponential parameters detailed in Table 1. All fits assume convolution with the cross-correlation function as an estimate of the IRF. A fit using just the four pure exponential components (three decays and a rise) in Table 1 is shown in Figure 1 (dashed line); the residuals from the fit are shown at the top of the plot. A Fourier transform of the residuals indicates a dominant oscillatory frequency of 105 cm^{-1}. This oscillation can be fit with a single cosinusoidal component damped by an exponential (solid line through residuals at top of plot); the solid line through the original data includes this cosine term. The oscillation period, phase, and damping time constants are 312 fs, 1.0 radians, and 450 fs, respectively. Figure 2 shows the isotropic fluorescence and the oscillation fit for the M2192 membranes. Here the sample is again excited at 860 nm; however, the fluorescence detected is centered at 943 nm. The membrane-bound preparation appears to have evidence for a second oscillatory component at ~20 cm^{-1}; the dominant fitted cosine term once again has a period of 312 fs, with a phase and damping time of 1.1 radians and 550 fs, respectively. Details of the pure exponential fitting parameters for both preparations as a function of excitation

TABLE 1: Isotropic Fits

sample	$\lambda_{ex}/\lambda_{det}$[a]	τ_{rise} (fs)	τ_1 (ps)	A_1 (%)	τ_2 (ps)	A_2 (%)	τ_3 (ps)	A_3 (%)
detergent-isolated LH-1	860/952 nm	90	0.55	27	5.6	40	~500	33
	850/956 nm	95	0.47	21	6.6	47	~500	32
M2192 membrane	860/943 nm	75	0.95	38	6.9	38	92	31
	870/955 nm	50	0.96	36	7.5	36	84	25

[a] λ_{ex} is the excitation wavelength; λ_{det} is the center wavelength of fluorescence detected by frequency upconversion. [b] Fit parameters defined in equation given in text.

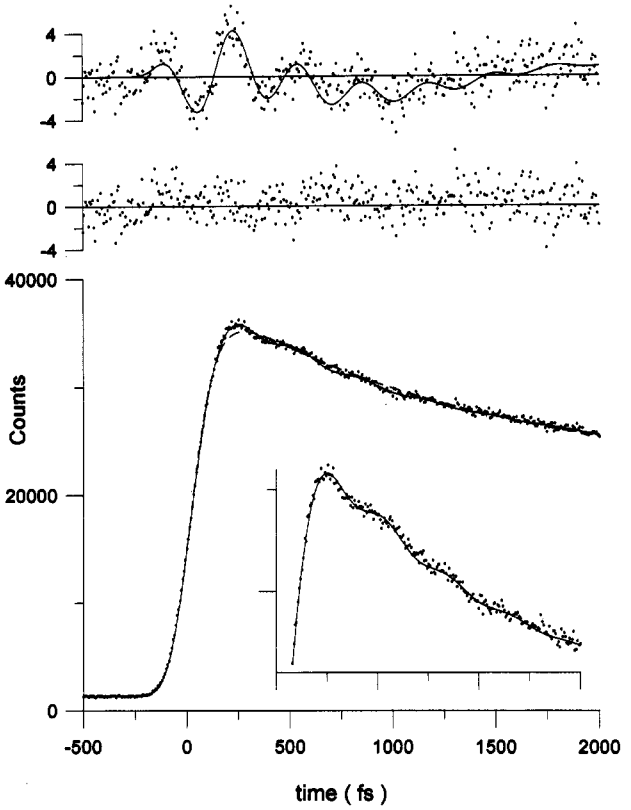

Figure 2. Time-resolved isotropic fluorescence from M2192 membranes excited at 860 nm and detected at 943 nm (dots) and fits (without cosine term, dashed; with cosine term, solid). Inset shows oscillations in more detail. (Top) Residuals to fit: upper panel shows residual to fit without cosinusoidal function and a line showing the cosine term that is added into the second fit form; the lower panel shows the residuals to full fit including cosine function.

wavelength are shown in Table 1. The excitation intensity is the same for all data sets, 0.4 nJ/pulse.

Figures 3 and 4 show the parallel and perpendicular signals (I_{par} and I_{perp}) for the detergent-isolated LH-1 and M2192 membrane preparations, respectively. Once again we show only the 860 nm excitation data. Both curves are simultaneously fit accounting for convolution with the IRF. The global fitting routine fits the coefficients of the following kinetic scheme describing the isotropic, $K(t)$, and anisotropic, $r(t)$, parts:[57]

$$K(t) = \sum_i \alpha_i \cos\left(2\pi\frac{t}{T_i} + \phi_i\right) e^{-t/\tau_i^{osc}} + \sum_j A_j e^{-t/\tau_j} - e^{-t/\tau_{rise}} \sum_j A_j$$

$$r(t) = r_\infty + \sum_j r_j e^{-t/\tau_j}$$

Typically $K(t)$ is determined by fitting the isotropic data independently (above) and fixing these coefficients for the simultaneous fit of I_{par} and I_{perp}. $K(t)$ includes the oscillatory

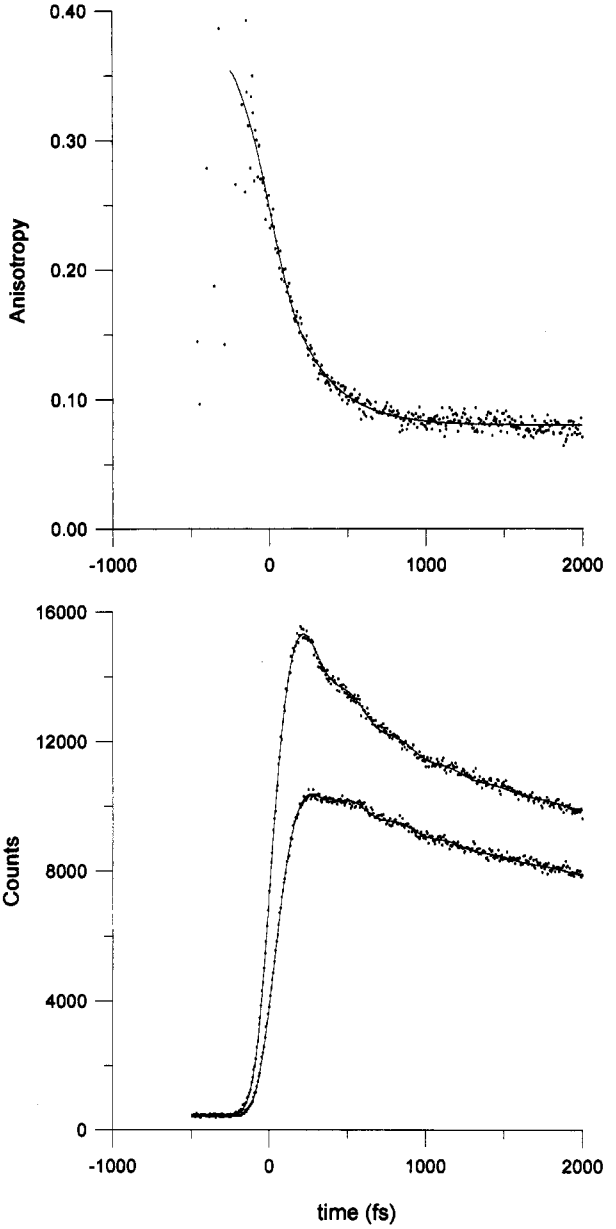

Figure 3. Fluorescence from M2192 membrane preparation LH-1 when excited at 860 nm and detected at 943 nm. Lower plot shows fluorescence parallel (upper curve) and perpendicular (lower curve) to the excitation pulse polarization; the data are shown in dots, and the respective fits, as solid lines. Data shown are sums of 10 scans of each polarization. The upper plot shows the raw experimental anisotropy function $R(t)$ (dots) and the same function derived from the fitted convoluted parallel and perpendicular curves (solid).

term(s) fit in Figures 1 and 2. We have chosen a simple model form for the anisotropy law $r(t)$: a sum of exponentials. The fits for $r(t)$ indicate a biphasic decay with a fast (~100 fs) and a slower (~400 fs) decay from an initial value of 0.38 (0.32 for detergent preparation) to a final value of about 0.07 (see Table 2). At the top of Figures 3 and 4 is shown the raw anisotropy, $R(t) = (I_{par} - I_{perp})/(I_{par} + 2I_{perp})$ from the

TABLE 2: Anisotropy Model from Simultaneous Fits to I_{par} and I_{perp}

sample	$\lambda_{ex}/\lambda_{det}$	r_1	τ_1 (fs)	r_2	τ_2 (fs)	r_∞
detergent-isolated LH-1	860/952 nm	0.14	110	0.11	370	0.07
	850/956 nm	0.17	110	0.07	520	0.06
M2192 membranes	860/943 nm	0.22	110	0.08	420	0.08
	870/955 nm	0.26	110	0.08	440	0.06

[a] Fit parameters defined in equation given in text.

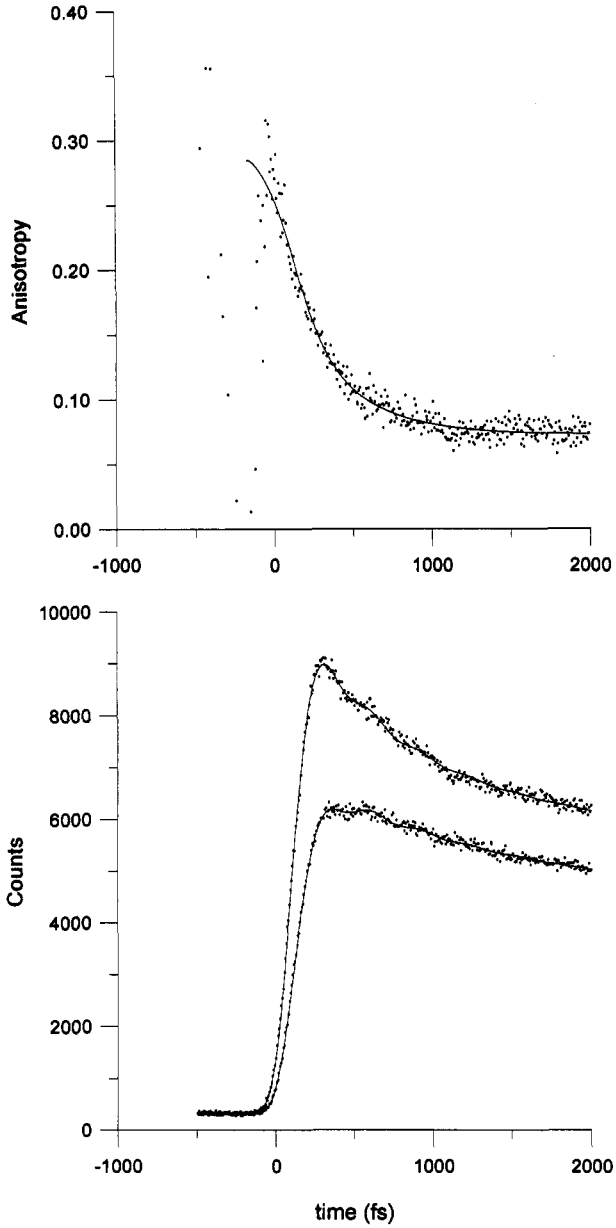

Figure 4. Fluorescence from detergent-isolated LH-1 complexes when excited at 860 nm and detected at 952 nm. Fluorescence parallel (upper) and perpendicular (lower) to the excitation pulse polarization (dots) and their respective fits (solid lines). The upper plot shows the raw experimental anisotropy function $R(t)$ (dots) and the same function derived from the fitted convoluted parallel and perpendicular curves (solid).

experimental data and this same quantity calculated from the convoluted fits to the parallel and perpendicular signal; this differs slightly from the real anisotropy function $r(t)$ extracted from the data.[57] The final anisotropy is consistent with earlier picosecond time resolved experiments[32] and the steady state fluorescence anisotropy.[11,58] The value for the initial anisotropy extracted from the data depends on the model form chosen for $r(t)$: the deviation between the fit and the data at earliest times indicates that even a two exponential component decay does not fit the data completely.

Experiments were performed with different excitation wavelengths on both preparations. In the case of M2192, we do not see evidence for significant wavelength variation of the depolarization process. In contrast, the detergent-isolated complexes show a more pronounced excitation wavelength dependence of the slower depolarization time constant. Limitations caused by the time resolution, signal-to-noise, and number of parameters in our fits discourage attempts to identify trends in the faster depolarization component. As regards the isotropic emission data, it can be said with reasonable confidence that the detergent preparation shows a longer rise time than the M2192. These two observations indicate that the detergent-isolated LH-1 may be spectrally more heterogeneous than the membrane preparation. It has been noted that the absorption spectrum of isolated LH-1 is wider than that of LH-1/RC chromatophores or the M2192.[28] Notice that the fluorescence rise time varies with excitation wavelength: the further to the red the antenna is excited, the faster the rise.

Annihilation Processes. The signal-to-noise requirements for the anisotropy measurements make it difficult to conduct experiments in the annihilation-free regime. Kinetic contributions due to both singlet−singlet and singlet−triplet annihilation will be present in the traces. We measured the kinetics of the singlet−singlet annihilation process separately by performing magic-angle measurements with a reduced repetition rate (250 kHz) to avoid accumulation of triplet states. These experiments were carried out on the detergent-isolated preparation only. The small size of the complexes allows the data to be interpreted within the simple puddle model for excitation energy transfer.[55] Figure 5 shows the results of the singlet−singlet annihilation experiments performed with the 250 kHz amplified laser system using four different excitation densities, together with numerical simulations of the data (described below). The traces have been normalized to the pulse energy to demonstrate the dramatic dependence of the lifetime on the pulse energy; for the highest pulse energy (6 nJ/pulse), >70% of the signal decays within the first picosecond. The ~6 ps component recorded in Figure 1 and Table 1 is absent in these scans and therefore is assigned to singlet−triplet annihilation. The experimental data show two effects: a fairly constant 1 ps fast decay and a varying ratio of this decay component to a long-lifetime component. The 1 ps component is still present at the lowest excitation density; we take this to be the lifetime for annihilation of two singlet excitations leading to one singlet excitation on the complex.

Since no analytical expressions are available for the nonlinear effects, we complemented the experiments with numerical simulations to check whether the absolute pulse energy dependence was consistent with singlet−singlet annihilation. Because the absorption of the sample was rather high, the variation of the intensity over the optical path had to be taken into account. The distribution of the absorbed energy per unit volume over the measuring volume was initially calculated using the measured optical density, path length, laser beam profile, pulse energy, and the BChl *a* extinction coefficient as input parameters. We assume the incident focused laser spot has a Gaussian

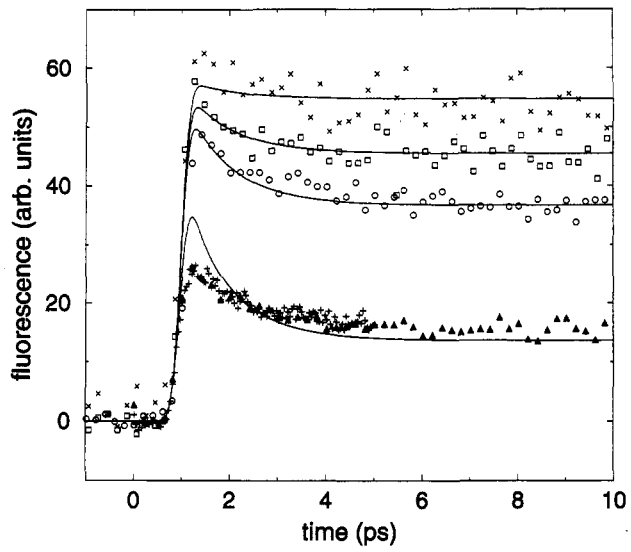

Figure 5. Energy dependence of the isotropic fluorescence with amplified laser experiment. The repetition rate for this measurement was 250 kHz with 200 fs pulses. The different traces correspond to pulse energies of (from top to bottom) 0.15 nJ (×), 0.6 nJ (□), 1.5 nJ (○), and 6 nJ (+,▲). The curves are the result of numerical simulations of singlet−singlet annihilation as described in the text. The experimental curves were normalized to the pulse energy; the 0.15 nJ curve was scaled arbitrarily since it was recorded at a different detection wavelength.

mode with a fwhm of 35 μm. The annihilation processes were then simulated for the calculated distribution of average energy density values (the kinetic scheme assumed for the annihilation process can be found in the Discussion section). The differential equations for the population of n-fold excited complexes[38,40,54] were integrated numerically assuming a Gaussian pump pulse of width 200 fs.[59] The lifetime of the decay process from double to single excited complex was taken to be 1 ps, as suggested by the experimental traces. The rates of the higher order annihilation processes were taken to be proportional to the square of the number of excitations involved. The size of the isolated complexes was assumed to be 16 pigments, slightly larger than what was deduced from electron microscopy pictures,[16] however, smaller than the size of the crystallized LH-2 complex[5] and half the size of the complexes shown in the projection maps of Karrasch *et al.*[17] The effect of ground state depletion during the pulse was included in the simulation of the dynamics by scaling the absorption cross sections of the complexes on the basis of the number of excited states. Here it was presumed that the excited state results in a bleaching corresponding to that of two pigments (see below), as suggested by the excited difference spectra measured for LH-1 and the isolated subunit (B820) of this antenna.[23] The weighted sum of traces was finally convolved with the gate laser pulse.

Figure 5 shows the results of the simulations superimposed on the experimental data points. The energy dependence is predicted rather well except at the highest energy density, where the simulation deviates from the data points. This is to be expected, however, as excited state absorption was ignored in the calculation. This is likely to be important at these pulse energies particularly as the excited state difference spectrum[23,26] at the pump wavelength is dominated by excited state absorption. Therefore, at very high excited state densities significant direct formation of double excited states will occur, resulting in very fast "annihilation" since no migration is involved in this loss process. Given the reasonable agreement between the remaining experimental data and the simulations and as the amplitudes of the annihilation decay component and the "natural" long lifetime depend mainly on the size of the complex, we conclude that the estimate of eight dimers per detergent-isolated complex is approximately correct. We can conclude with more certainty that the predominant fast annihilation process at the excitation energies used in the anisotropy measurements (0.4 nJ/pulse) is indeed $2 \rightarrow 1$ singlet−singlet annihilation. We note that there is a variation in the fitted time constant of this decay component between the low and high repetition rate experiments; we take the time constant from the low repetition rate experiment of ~1 ps as more representative due to inherent problems of extracting multiple exponential decay components in the high repetition rate data. We interpret the meaning of the 1 ps annihilation time in the Discussion section.

The high repetition rate experiments show an additional decay component due to S−T annihilation. The accumulation of triplets is presumably on the carotenoid molecules present in the LH-1 antenna.[60] The interpretation of the ~6 ps lifetime in the isolated complexes is rather straightforward. Given the 1 ps S−S annihilation time, we can conclude that the 6 ps S−T annihilation process in these small complexes is not migration limited and can be described by the trapping-limited "puddle" model.[55] This implies that the decay process is dominated by a decay time equal to the number of dimers times the S−T decay time that would be observed for a single dimer (with an associated triplet carotenoid),

$$\tau_{S-T} \cong N\tau_{decay}$$

Direct comparison with other experiments is not possible, as this is the first instance that this process has been time-resolved. However, Monger *et al.* measured the fluorescence quantum yield in membranes of *Rs. rubrum* (at room temperature) as a function of the triplet concentration and concluded that carotenoid triplet states are approximately 2 times more effective as singlet quenchers than open RCs.[56] However, the S−T annihilation experiments of Monger *et al.* were not performed with homogeneous illumination, and the annihilation efficiency was probably underestimated. Measurements performed at 77 K (under homogeneous illumination conditions) indicated that the carotenoid triplets were approximately 4 times more efficient quenchers than open reaction centers[22] or a S−T decay time of 12 ps (since the trapping time in *Rs. rubrum* is ~50 ps[33,34]). After taking the differences in size into account, this last value comes closest to the lifetime found here. The values of van Mourik *et al.*[22] correspond to a lifetime of ~12 ps for an antenna size of 12 dimers, or $\tau_{decay} = 1$ ps (ignoring the migration time); the data presented here correspond with $\tau_{decay} = 0.75$ ps (assuming a complex size of eight dimers). Due to the difference in temperature, the two experiments are not directly comparable; however, the comparison does support our assignment of the 6 ps lifetime to S−T annihilation.

For the isolated complexes we can also check the amplitude of the S−T annihilation lifetime. Since annihilation is very efficient in these small domains, we only have to consider complexes with zero or one triplet excitation. If we ignore S−S annihilation for the moment, then due to the high repetition rate, a steady state triplet concentration will form according to

$$\frac{dn^T}{dt} = \phi F x(1 - n^T) - n^T K^T = 0$$

Here n^T is the fraction of complexes with a triplet carotenoid, F is the repetition rate of the laser (8×10^7 s^{-1}), ϕ is the yield of triplet formation, x is the fraction of excited complexes per pulse (about 20% in the 0.4 nJ experiments), and K^T is the decay

rate of the triplet states. In the experiments the amplitude of the 6 ps lifetime is 40−50%, suggesting that $n^T = 0.45$ and that $K^T/\phi = 2 \times 10^7$. For a triplet lifetime of 3 ms,[60] this would correspond with a triplet yield of ~1.5%. This is about a factor of 3 less than expected on the basis of the average singlet lifetime and triplet yield observed in other BChl *a* antennae.[14] This yield is not unreasonable however since we have ignored singlet−singlet annihilation both in consideration of this average singlet lifetime and in ignoring the competition between both S−S and S−T annihilation in some complexes. It therefore appears that the amplitude and time constant of the intermediate decay in the isolated complex data are consistent with singlet−triplet annihilation. Notice that the estimate of $n^T \sim 0.45$ indicates that there is a higher probability of finding a triplet excitation than a singlet on a given complex under the conditions of high repetition rate pumping.

In the chromatophore measurement the annihilation kinetics are much more complicated. The M2192 membranes are large pools of hundreds of pigments[61,62] probably containing circular domains; however, these domains are not isolated from each other as is the case in the detergent preparation. There is also likely to be heterogeneity in the sizes of the overall pools. Therefore, annihilation processes will occur within circular domains and between domains. The prominent contribution of a 1 ps lifetime (30−40%), and the clear difference with the "next" lifetime, indicates that the excitation migration is fast within small domains (of size similar to our isolated complexes) and that hopping between domains is about 1 order of magnitude slower. Note that it is not correct to compare the intermediate lifetimes of isolated complexes and membranes in Table 1. Due to the much shorter average lifetimes in the membranes, the yield, and therefore accumulation, of triplet states is much smaller than in the isolated complexes. Therefore, the 7 ps lifetime in the membranes is probably predominantly due to S−S annihilation.

Discussion

In this work the femtosecond depolarization of the spontaneous emission in the light-harvesting core antenna of a photosynthetic purple bacteria has been observed for the first time. The depolarization occurs nonexponentially, with characteristic times of ~100 and ~400 fs (from a biexponential fit), and this depolarization is ascribed to excitation energy transfer among differently oriented BChl *a* molecules within the core antenna. In the following we will discuss (1) the anisotropy decay and (2) the fluorescence lifetime in these experiments and (3) the origin of the oscillations in the isotropic fluorescence. We will discuss the connection between the anisotropy decay and annihilation kinetics in terms of two classes of structural models involving circular arrangements of BChl *a* dimers. Finally we will evaluate the use of the incoherent hopping model for the description of energy transfer in the antenna and discuss the relationship between this and previously proposed exciton models.

The Anisotropy Decay. The anisotropy decay obtained from the experiment cannot be directly interpreted in terms of a rate of energy transfer since this relationship is model dependent. In the following we will interpret our data in terms of two types of model, outlined schematically in Figure 6 and strongly related to the competing structural predictions for LH-1.[8,9,17] Common to both models is that the transition dipoles of the pigments are oriented within the plane/membrane, as is well established by polarized light spectroscopy.[11,58] Clearly the choice of ring models is motivated by the observation that the BChl pigments are arranged in circles in the crystal structures of LH-1[17] and

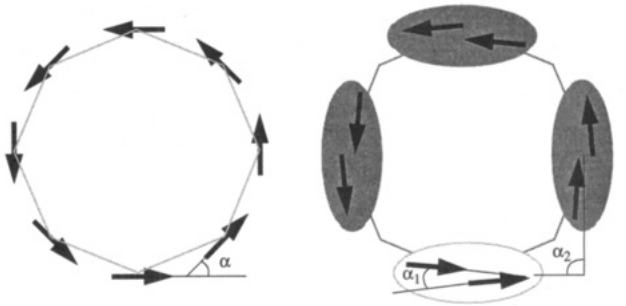

Model A Model B

Figure 6. Models for the pigment organization for the discussion of the annihilation and depolarization data (see text). Each solid arrow represents the major transition dipole of a bacteriochlorophyll dimer. Model A has transition dipoles arranged symmetrically in a ring. Model B has two structural domains with clusters of two dimers arranged symmetrically on a circle.

LH-2.[5] The orientation of the dipoles must be uniformly distributed within the plane, otherwise residual anisotropies larger than 0.1 are predicted. In addition to considering two structural models, the uncertainty in the number of sites (overall ring size) must be addressed. *For both models each site is assumed to be a BChl dimer.*

In the first model (A in Figure 6), the dimers are organized on a circle and all spacings and angles are equal. (α is the angle between nearest neighbor dimer transition dipoles.) This model yields a single-exponential decay of the anisotropy, from 0.4 to 0.1, with a characteristic decay time of

$$\frac{\tau_{hop}}{4(1 - \cos^2 \alpha)}$$

where $\alpha = 360°/N$, if all N sites are equivalent and only nearest neighbor hopping is considered (see Table 3). τ_{hop} is defined as the inverse of the nearest neighbor pairwise transfer rate. Nonexponential anisotropy decay is introduced by incorporating a distribution of hopping rates due to the inhomogeneous nature of the antenna. Simulations of this effect (below) show that a modest inhomogeneous distribution of the site energy is sufficient to account for the observed nonexponential decay. In the second model, pigment clustering occurs (model B in Figure 6); this gives rise immediately to two anisotropy decay time scales in the absence of any spectral inhomogeneity. In this model, equilibration between the two sites within a cluster gives rise to an initial drop in anisotropy of

$$\Delta r = 0.2 + 0.1(1 - 3 \cos^2 \alpha_1)$$

The remainder of the depolarization takes place due to intercluster excitation transfer. In the most extreme case of $\alpha_1 = 90°$, the final anisotropy of 0.1 is already reached by equilibration within the subcluster. This model can alternatively be thought of as a tetramer model: the important aspect is that depolarization occurs on two time scales. The precise nature of the processes within the clusters is not important: it can be hopping between dimers or dephasing between tetrameric exciton levels.[49]

Model A: Symmetric Rings. The effect of inhomogeneity in the first model has been tested by simulations assuming Förster energy transfer between dimers. We will comment on whether incoherent transfer between dimers is justified later in the discussion. Two ring sizes are considered: $N = 16$ for direct comparison with the reassociated LH-1 structure inferred from

TABLE 3: Relation between Depolarization and Migration-Limited Annihilation Times

number of sites (N), angle α	depolarization time (model A)	migration time for S−S annihilation	maximal hopping time from annihilation (ps)	calculated depolarization time (ps)
3, 120°	0.333 τ_{hop}	0.375 τ_{hop}	<2.7	<0.89
4, 90°	0.250 τ_{hop}	0.625 τ_{hop}	<1.6	<0.40
6, 60°	0.333 τ_{hop}	1.46 τ_{hop}	<0.69	<0.23
8, 45°	0.500 τ_{hop}	2.63 τ_{hop}	<0.38	<0.19
10, 36°	0.724 τ_{hop}	4.13 τ_{hop}	<0.24	<0.18
12, 30°	1.000 τ_{hop}	5.96 τ_{hop}	<0.17	<0.17
14, 25.7°	1.328 τ_{hop}	8.13 τ_{hop}	<0.12	<0.16
16, 22.5°	1.707 τ_{hop}	10.6 τ_{hop}	<0.094	<0.16
18, 20°	2.137 τ_{hop}	13.5 τ_{hop}	<0.074	<0.16

the data of Karrasch *et al.* and $N = 8$ for the smaller detergent-isolated LH-1 complexes. The number of sites is chosen to be eight in the latter case on the basis of size estimates for isolated complexes[16,44] and the singlet−singlet annihilation simulations in the previous section. Each dimer site energy is selected by a Monte Carlo scheme from a Gaussian inhomogeneous distribution function. The pairwise energy transfer rate is calculated between all sites assuming Gaussian[63] homogeneous lineshapes for the spectral overlap term,[64] with distances and orientation factors, κ^2, appropriate for the N site ring structure. In the LH-2 structure the BChl *a* molecules (and thus the transition dipoles) are seen to be tilted with respect to the ring tangent;[5] as the degree of ring tilt is not known for LH-1, we have assumed the dimer transition dipoles to be oriented tangential to the ring as shown in Figure 6; this affects only the κ^2 values used to calculate the Förster rate. *Ad hoc* detailed balance and symmetrization is applied to the Förster formulation, as in ref 65. Solution of the Pauli master equation for the population on each of the N dimer sites is achieved numerically. The overall fluorescence follows the total population dynamics; this is constant (except for the long natural decay: annihilation effects are not included), as the calculation assumes that the probability of excitation and detection of a given dimer is independent of wavelength. The depolarization dynamics are calculated numerically by angle averaging using the methodology suggested by Magde.[66] Averaging over 5000 Monte Carlo iterations yields a converged depolarization decay.

In all the simulations that follow we have assumed a fixed homogeneous linewidth (250 cm^{-1} fwhm) and a 66 cm^{-1} Stokes shift for each dimer.[23] This estimate of the homogeneous linewidth is consistent with room temperature photon echo results on the B800 band of LH-2 from our laboratory.[63] The integrated transition dipole strength of the dimer transition is taken to be 77 D^2.[67] Van Mourik assumed the inhomogeneous broadening of the LH-1 band in detergent complexes at 4 K to be ~250 cm^{-1} fwhm,[44] whereas hole-burning studies of LH-1 chromatophores by Reddy *et al.* found a much smaller effective inhomogeneity (80 cm^{-1}).[25] Hole burning in the isolated B820 subunit indicated ~320 cm^{-1} inhomogeneity.[42] We have thus considered inhomogeneous distribution function widths of 0, 250, and 500 cm^{-1} fwhm and *fixed the homogeneous linewidth* to illustrate the effect on the anisotropy decay of varying just one parameter. The overall linewidth is therefore not consistent with the experimental absorption spectrum at 300 K for every simulation.

Figure 7 shows the result of a 300 K simulation for the 16 dimer ring structure as seen in the electron diffraction projection map of Karrasch *et al.*[17] A 12−16 dimer ring is currently proposed as the best model of the *in vivo* LH-1 antenna surrounding the reaction center and is probably a good representation of M2192 chromatophores (as suggested in ref 43). The dimer center-to-center distance is estimated at 18.6 Å directly from the projection map, which shows the chromophores arranged on a circle of radius 48 Å.[17] For comparison, the LH-2 structure of McDermot *et al.*[5] would give an interdimer spacing of 17.8 Å. Förster theory predicts a nearest neighbor dimer-to-dimer hopping time of 80 fs for a homogeneous antenna with the Karrasch *et al.* structure. This gives rise to a depolarization time scale that is in fairly close agreement with experiment, as seen in Figure 7; this is significant, as no Förster parameters have been adjusted and all geometric factors come from ref 17. The results of the Monte Carlo simulation show that with just 250 cm^{-1} inhomogeneity, 30% of the anisotropy decay becomes slow (500 fs). In addition the initial rate of depolarization is somewhat slower (150 fs) than for the homogeneous antenna. When a 500 cm^{-1} inhomogeneity is considered, the slow component now has a larger amplitude than the fast. If these simulations are compared with the M2192 biexponential experimental decay data, clearly an inhomogeneity ~250 cm^{-1} gives the best agreement. We note that neither the higher overall connectivity of M2192 chromatophores nor the possibility for variation in ring size within the M2192 membrane has been included in this simulation. However, very recent upconversion experiments in our laboratory with LH-1/RC chromatophores[68] indicate very similar depolarization dynamics compared to M2192, indicating that these issues may not be that significant. The value found here for the M2192 site inhomogeneity need not be inconsistent with the 80 cm^{-1} inhomogeneous linewidth from 4 K hole burning (see below).

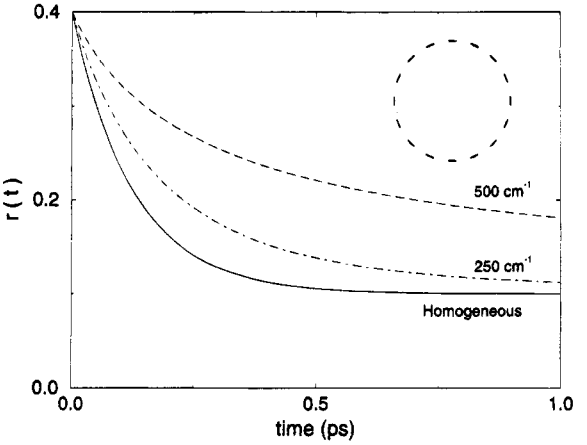

Figure 7. Effect of inhomogeneous distribution function on the depolarization of a 16-dimer ring. Förster hopping between BChl *a* dimers assuming 96 Å ring diameter (consistent with ref 17) in arrangement shown in Figure 6 (model A). Homogeneous decay (solid line) single exponential with 126 fs time constant; inhomogeneous distribution function with fwhm 250 and 500 cm^{-1} simulations fit to biexponential 150 fs (71%), 500 fs (29%) and 165 fs (43%), 1.4 ps (57%), respectively.

Figure 8 shows the results of a similar simulation for an eight dimer ring. This simulation is relevant to the smaller detergent-isolated complexes. However in this calculation we have not simply scaled the $N = 16$ ring geometry indicated in the electron diffraction map to eight dimers; if this is done, the depolarization

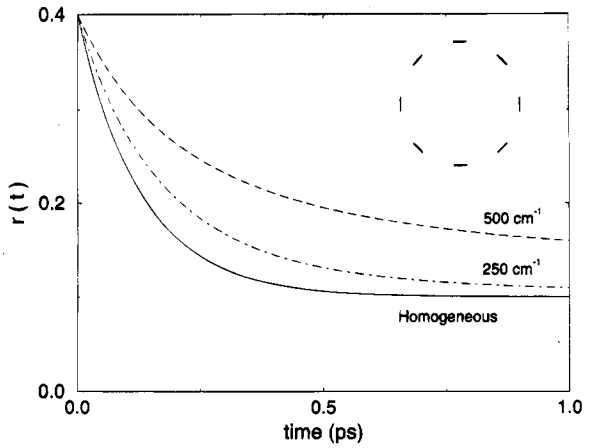

Figure 8. Effect of inhomogeneous distribution function on the depolarization of an eight-dimer ring. Förster hopping between BChl *a* dimers assuming 58 Å ring diameter in arrangement shown in Figure 6 (model A). Homogeneous decay (solid line) single exponential with 129 fs time constant; inhomogeneous distribution function with fwhm 250 and 500 cm^{-1} simulations fit to biexponential 160 fs (84%), 600 fs (16%) and 190 fs (60%), 1.4 ps (40%), respectively.

time scale is much too fast (consider Table 3). For the calculation shown in Figure 8, the interdimer separation was chosen to be 22.3 Å, to yield a homogeneous depolarization characterized by a 130 fs time constant. The nearest neighbor hopping time is now 265 fs. In comparison to the 16-fold ring, the same magnitude inhomogeneity here introduces a less significant slower phase: for 250 cm^{-1} inhomogeneity only 16% of the anisotropy decay is slow (605 fs). To reproduce the ratio of slow to fast depolarization amplitudes experimentally observed for the detergent complexes (Table 2) requires an inhomogeneity closer to 500 cm^{-1}. In this case the overall absorption linewidth comes into agreement with the experimental width (580 cm^{-1}), and the inhomogeneity is consistent with the conclusions of Visser *et al.*'s simulations of time-resolved spectral equilibration for *Rs. rubrum* LH-1.[23] A more thorough "fit" to the data of the simulation time scales and amplitudes, for either the M2192 or the isolated complexes, is not warranted because the inclusion of the spectral selection imposed by both excitation and detection is necessary to fully mimic the experiment. This will be treated in a future paper.[69]

The consideration of inhomogeneity in the antenna allows an explanation of several other aspects of the experimental data. The initial values for the fitted anisotropy functions (Table 2) are close to but slightly smaller than the expected 0.4. To avoid contamination of the parallel signal with upconverted scattered light in the experiment, we have to detect the fluorescence in the red wing of the emission spectrum. A consequence of this detection wavelength is that we put a bias on detection toward fluorescence events which occur after an energy-transfer event, since for an inhomogeneous antenna energy transfer gives a red-shift in the emission spectrum. This red shifting is partly observed in the ~70 fs rise time of the isotropic fluorescence. Consistent with this explanation is the observation in the data that the deviation from $r(0) = 0.4$ is greater the bluer the excitation wavelength. Further, we notice that the final values of the anisotropy are lower than 0.1, the value expected for equilibration amongst dipoles in a plane. The effect of spectral selecting pigments excited in the blue end of the band and detecting the reddest pigments also gives rise to final anisotropies below 0.1.[69] Finally, as we noted earlier, differences in the degree of inhomogeneous broadening in the antenna between membranes and detergent-isolated complexes are likely responsible for the slower isotropic rise times and more dispersive depolarization for the detergent preparation. This interpretation is sensitive to the overall connectivity and complex size assumed for the membrane antenna.

Model B: Clustered Dimers. Turning our attention to the second pigment arrangement shown in Figure 6, interpreting the biexponential decay in this model is fairly simple. The data fits indicate an angle between the transition dipoles within a cluster of $\alpha_1 = \sim 30-60°$ (depending on the amplitude of the fast component) and an intracluster equilibration time of ~100 fs. The interpretation of the second lifetime then depends on the angle α_2 and N (now the number of *clusters* in the ring). For $\alpha_2 = 90°$ and $N = 4$, the observed 400 fs lifetime corresponds to a cluster-to-cluster hopping time of 1.6 ps. These values extracted for the hopping time are quite markedly different than those consistent with model A. In the following section we examine whether the hopping times emerging from either of the two models are consistent with the observed annihilation rates for the isolated LH-1 complexes.

The Excited State Lifetime: Annihilation Processes. We have seen that the fluorescence lifetimes in the experiments display fast decay components as a result of singlet−singlet and singlet−triplet annihilation. Although this is a complication for the analysis of the anisotropy decay, additional information about the energy migration can be obtained from these short components. Moreover, the time-resolved annihilation in the antenna measured here allows for comparison with older annihilation experiments where time-integrated fluorescence yields were used as a measure for annihilation processes.[38,39,61,62] Singlet−singlet annihilation studies have so far assumed rather slow hopping (0.5−1 ps) within a domain[38,39] and very efficient decay; that is, the annihilation process was presumed to be migration limited. The recent finding of hopping times on the order of 100 fs in this work and elsewhere[23] changes this picture somewhat. These very fast hopping times might make it rather unrealistic to presume migration limited annihilation.[40]

Earlier we assigned the 1 ps component as the 2 → 1 "annihilation lifetime"; let us consider what this time constant means. We assume the following kinetic scheme:[40,70]

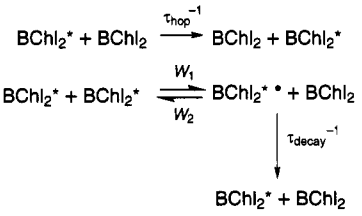

The overall 2 → 1 exciton annihilation process can be approximated as an exponential decay with a lifetime that is proportional to the sum of the migration time of excitations in the domain and the effective trapping time[70]

$$\tau_{ann} = \tau_{mig} + \tau_S$$

$$\tau_S = N\tau_{relax} = N\tau_{decay}(W_2/W_1)$$

For the circular model the migration term can be written as[71]

$$\tau_{mig} = \frac{N^2 - 1}{24}\tau_{hop}$$

Here N is the number of sites (dimers), and τ_{hop} is the hopping time (we are so far assuming all sites are identical). τ_s is the effective trapping time;[40,70] τ_{relax} is the equilibrated relaxation time of the doubly excited state, where W_2 is the rate of decay of this state back to two singly excited dimers, W_1 is the rate of the reverse process, and τ_{decay} is the radiationless decay time of

the dimer from the doubly to singly excited state. For example, for a symmetric ring with eight sites, $\tau_{mig} = 2.63\ \tau_{hop}$. If we assume $W_1 = W_2$ and choose a reasonable internal conversion time, $\tau_{decay} = 75$ fs, the observed 1 ps annihilation time corresponds to an average hopping time of 153 fs. If, on the other hand, we consider the limiting case of $\tau_s = 0$, this yields the slowest hopping time that is allowed by the 1 ps annihilation time, $\tau_{hop} = 382$ fs.

The above expressions neglect the inhomogeneous nature of the antenna. Inhomogeneity probably has little effect on the room temperature migration time,[72] but it does have a pronounced effect on the effective trapping time. For an inhomogeneous system τ_s will shorten due to an effective concentration of the excitations on the lower energy pigments. A rough estimate of this effect yields a factor of ~2 for the values of the inhomogeneous distribution used in the anisotropy simulations above. Overall the impact of inhomogeneity in the antenna would appear to be that the trapping speeds up while the migration is somewhat slowed down. It is therefore reasonable that for a moderately fast τ_{decay} within an inhomogeneous antenna that the annihilation time is after all dominated by exciton migration. Table 3 is therefore constructed to show the longest possible hopping times consistent with the 1 ps annihilation decay, i.e. assuming $\tau_S = 0$, as a function of ring size. It can be seen that interpretation of the annihilation decay for circular complexes of different sizes yields strongly varying hopping times; the simulations to the S−S annihilation data shown in Figure 5 are fairly sensitive to the assumed N, but values of N between 6 and 12 are possible.

Recall that for a ring of dimers with $N = 8$ the annihilation time of 1 ps limits the hopping time to $\tau_{hop} < 382$ fs. In the absence of spectral inhomogeneity this implies a depolarization time faster than 190 fs. The dominant experimental depolarization time scale is indeed consistent with this, and the assumed homogeneous hopping time in the inhomogeneous anisotropy simulation, Figure 8, is also consistent with this inequality. Table 3 shows that all circular arrangements of the transition dipole moments with $N > 6$ allow agreement between the depolarization and annihilation data.

Let us briefly consider the spatially clustered pigment arrangement, model B, in this regard. The annihilation process and the slow phase of the anisotropy decay will be dominated by hopping between clusters. If we thus treat the complex as four "super molecules", in the sense that annihilation within a cluster is much faster than the intercluster hopping time, the annihilation parameters reduce to $N = 4$, $\tau_{mig} = 0.625\ \tau_{hop}$. The 1 ps annihilation decay time implies a 1.6 ps cluster−cluster hopping time if $\tau_S = 0$ for the tetramer (Table 3). This upper limit on the hopping time is in agreement with the number deduced from the slow phase of the anisotropy decay (400 fs) assuming $\alpha_2 = 90°$. Table 3 indicates that for model B only complexes with three or four tetramers are consistent with both sets of data.

So far we have considered the effects of depolarization and annihilation in the antenna separately. One might consider how, if at all, the annihilation kinetics and the steady state triplet population affect the photoselection and anisotropy decay. Fortunately, the effects of annihilation on the fluorescence anisotropy are small for transition dipoles equally distributed in orientation within a plane.[73] The theoretical effect of annihilation on the residual anisotropy is about 5−10% for the excitation densities at hand (0.4 nJ).[73] Therefore, the amplitude of the kinetic contribution to the depolarization is probably small. Moreover, the annihilation process is about 10 times slower than the fastest depolarization component and therefore cannot have a strong influence on the early anisotropy dynamics.

Oscillations in the Isotropic Fluorescence: Beats in the Excited State. The observation that the oscillations observed in the isotropic decays are not present in the anisotropy would seem to suggest that the beats arise from vibrational motion. The bandwidth of the laser is sufficient to impulsively excite a mode with a 105 cm^{-1} frequency. The beat frequency recovered in all four experiments with both sample preparations is 105 cm^{-1}. This frequency is in agreement with the dominant room temperature beat (110 cm^{-1}) in the pump−probe data of Chachisvilis *et al.*[50] However, the observations of beats in the fluorescence shows that the nuclear wave packets probed are in the chromophore's excited state. Various time and frequency domain measurements reveal similar frequencies for BChl *a* dimers but not for monomers. Savikhin and Struve detect no oscillations in bacteriochlorophyll monomer in dilute solution via the femtosecond pump−probe technique.[74] In contrast, for the special pair in the reaction center of *Rb. sphaeroides* the dominant beat frequencies recovered by Vos *et al.* from oscillations in pump−probe data are 92, 122, and 153 cm^{-1}.[51] Stanley and Boxer report similar oscillation frequencies in fluorescence upconversion experiments on the special pair,[52] confirming Vos *et al.*'s claim that a large part of the vibrational motion impulsively excited in the reaction center is, like that observed here, in the excited state. In the frequency domain, Small and co-workers find evidence for a single "marker mode" with frequency of 115 cm^{-1} in low temperature hole burning of the special pair band of the reaction center.[75] Likewise, in the resonance Raman spectra, no strong vibrational bands below 177 cm^{-1} are found in the (monomeric) accessory bacteriochlorophyll in reaction centers whereas for the special pair, bands observed at 128, 95, 71, and 34 cm^{-1} are attributed to BChl *a* dimer formation.[76] These Raman frequencies correspond, of course, to ground state vibrations but indicate that these modes are strongly coupled to the electronic transition.

The observed LH-1 beat frequency in this and the work of Sundström's group seems strong corroborating evidence that the chromophore in LH-1 is indeed a bacteriochlorophyll dimer. It should be noted however that Reddy and Small do not resolve a signature for this excited state vibration in hole-burning spectra of LH-1,[25] in contrast to their group's measurements on the reaction center.[75] A further contrast is found for *Rb. sphaeroides* LH-2. Contrary to expectations from the X-ray structure,[5] which shows the B800 BChl *a* to be monomeric, the B800 band shows weak beats in the time-resolved transient grating at room temperature.[63] The B850 band of LH-2 appears to show much weaker beats than the B875 band in LH-1; in the room temperature time-resolved fluorescence none are observed,[77] and the beats are far less pronounced at low temperature in pump−probe data as compared to LH-1.[50] This last observation seems consistent with the structural observation that the B850 excited state is more likely to be delocalized over more than one Bchl *a* dimer. We conclude that the 105 cm^{-1} mode probably corresponds to a dimer intramolecular vibration in the excited state.

The dephasing time of the 105 cm^{-1} oscillation is found to be ~300−500 fs (Figures 1 and 2). The exact value is hard to recover from the fits, as the rise time and the oscillation parameters are strongly correlated in the fit. A ~300 fs dephasing time is comparable to that reported by Chachisvilis *et al.* from linewidths in the Fourier transform of pump−probe fit residuals.[50] However, the process of transforming the residuals cannot be regarded as a quantitative procedure to determine the oscillation dephasing, as the least squares

exponential fitting algorithm will distort any real damped oscillation to improve the fit in the absence of oscillatory functions. Both Vos *et al.*[51,78,79] and Chachisvilis *et al.*[50] have found the oscillation damping rate is temperature independent over a range of ~10−295 K. Vos *et al.* observed that the oscillations are more pronounced (and the dephasing somewhat slower) in membrane than in detergent-isolated RC complexes.[78] They interpreted these two results as indicating that the pure vibrational dephasing rate is very slow and that the damping time of the observed oscillation is in fact governed by site inhomogeneity in the vibrational frequency. Our experiments also indicate a slower oscillation damping time for antennae in the native membrane environment (which we know to be electronically more homogeneous than the detergent-isolated antenna).

In our analysis of the depolarization and annihilation kinetics, average hopping times on the order of 260 fs ($N = 8$) or 80 fs ($N = 16$) are consistent with the data when the model of a symmetric circular arrangement of dimers is used. This implies that the residence time on a single pigment is <130 fs ($\tau_{hop}/2$ for two nearest neighbors). The observation that the excited state nuclear wave-packet dephasing time (>300 fs) in LH-1 appears to be longer than this residence time, in the context of model A, raises the interesting possibility of vibrational coherence transfer.[80−83] Jean and Fleming have shown that coherence transfer can give rise to nuclear coherence dephasing on a time scale much longer than suggested by naive application of the Bloch equations,[83] *i.e.* that slow dephasing of the vibrational coherence is possible in the case where the electronic population relaxation time is very short. The fact that no oscillations in the anisotropy are observed in our data is consistent with the electronic coherence of the antenna excited state being lost very fast.[84−86] In contrast, applying the model B structure, one could simplistically associate the vibrational coherence damping with the longer cluster residence time (cluster−cluster hopping time ~1.6 ps; residence time ~800 fs) and need not invoke coherence transfer. However, a more detailed description of the electronic coupling within the tetramer cluster would be required to evaluate whether other vibrational dephasing time scales should be detected in the signal.

The 20 cm^{-1} oscillatory component in the M2192 data included in our fit, although recovered in Chachisvilis *et al.*'s LH-1 data also,[50] may be an artifact due to the fitting of a correspondingly short time range dataset (less than one full oscillation period). Likewise the rise times recovered (Table 1) are extremely difficult to analyze due to the multiple effects taking place in the early time signals. Spectral equilibration will certainly lead to some rise in the red edge of the fluorescence spectrum; however, simulations suggest that the amplitude of the rise will not be greater than 50%. The magnitude of the effect of equilibration on the kinetics depends on the derivative of the emission spectrum at the wavelength of observation, since the equilibration corresponds with a red-shift of the emission spectrum. Similar measurements performed in the red tail of the chlorophyll emission spectrum of algal LHC-II see minimal (or confusing) effects from the equilibration on the rise component of the isotropic fluorescence.[87] Wave-packet motion, as witnessed by the oscillations, will also lead to a delay in the peak fluorescence, and high-order singlet−singlet annihilation events (that are nonlinear with the pulse temporal profile) also contribute to the shape of the rising edge.

Localized vs Delocalized Models. Thus far we have discussed our experimental results in terms of electronic states localized on individual dimers, with weak coupling between adjacent dimers. This interpretation may be oversimplified. Structural and spectroscopic information on LH-1 may be interpreted so as to yield a model in which the coupling strength between dimers may be comparable to the intradimer coupling strength. In this section we will examine the structural and spectroscopic arguments.

The recently determined crystal structure of LH-2 shows the B850 chromophores to be arranged in an almost perfect circle of 18 BChl *a* molecules.[5] The closest distance between BChl rings bound to the same $\alpha\beta$ is 3.4−3.5 Å, whereas between BChl rings on neighboring $\alpha\beta$ units the distance is 3.8−3.9 Å.[88] The overlapping molecular orbitals facilitate strong exchange interactions[89] between pigments within an $\alpha\beta$ pair, resulting in some charge-transfer character of the excited state, similar to that observed for the special pair of the RC.[90,91] Indeed, the B850 band was shown to have a very intense and anomalous Stark spectrum, similar to that of the special pair.[91] Nevertheless, there are two main reasons why these structural characteristics may result in localized states. (1) At these very short distances, in which the chlorin ring planes are in van der Waals contact, the majority of the interaction energy may result from non-Coulombic interactions with a very strong dependence on separation.[89] Therefore, the interaction energy within the $\alpha\beta$ dimer can greatly exceed the interdimer interaction energy. Using an exponential falloff and parameters from ref 92 we calculate the interdimer interaction energy to be ~2 times smaller assuming the distance of closest approach of the two rings. With an intradimer coupling, $|V|$ ~230 cm^{-1},[21] this means interdimer coupling is 110 cm^{-1} or less. This effect will be more pronounced for LH-1, where it is suspected that the intradimer and interdimer separations are more distinguishable.[17] In an exciton model, this will give rise to two discrete sub-bands which correspond to dimer upper and lower exciton eigenstates (two Davydov components).[49] In the absence of site inhomogeneity the states in the lower sub-band, for example, will be delocalized combinations of the lower dimer component. (2) There appears to be significant inhomogeneous broadening (>250 cm^{-1}), however, in the isolated B820 subunit at low temperatures.[42,43] If we conservatively assume an energetic disorder amongst the chromophores making up the intact antenna comparable to the interdimer coupling strength, *i.e.* 100−200 cm^{-1} fwhm, the excitonic eigenstates become much more localized, although the upper and lower bands remain.[49,93] We note here that in our experiments we excite only into the lower dimer band.

The results of hole-burning experiments performed by Reddy *et al.* on LH-1 have been, in contrast, interpreted as evidence for excitations delocalized over a large number of pigments.[25,94] Narrow holes could only be burnt in the red wing of the LH-1 absorption band. This was ascribed to the presence of the lowest energy exciton ($k = 0$) state in this spectral region. Reddy *et al.* argue that this state has oscillator strength as a result of the pigment spectral inhomogeneity.[25] The broad feature in the center of the B875 band is attributed to higher exciton states, which undergo rapid relaxation. They report an inhomogeneous width of only 80 cm^{-1}. These experiments are performed at low temperatures (4 K) in order to minimize the effect of pure dephasing. In this limit, inhomogeneity leads to reduced exciton delocalization and the absorption spectrum will exhibit a reduced linewidth ("the effective inhomogeneous linewidth") as compared to the site inhomogeneous distribution width:[93] this is often referred to as motional narrowing. Following Fidder *et al.*,[93] we calculate that a monomer site inhomogeneous distribution of 200 cm^{-1} fwhm, with intra- and interdimer couplings of 230 and 110 cm^{-1}, respectively, will lead to an effective inhomo-

geneous linewidth, in the $k = 0$ state for example, of $\sim$70 cm^{-1}. Hence, our earlier estimate for the inhomogeneous distribution width may not be inconsistent with the hole-burning results. In addition, we note that Loppnow *et al.* have observed an almost 3-fold increase in the inhomogeneous broadening in rhodopsin and bacteriorhodopsin from 1.5 K to room temperature.[95] Having stated that the exciton may be still somewhat delocalized at low temperatures, we believe that the situation at room temperature is likely to be quite different. Phonons due to the protein environment, which are quiescent at low temperatures, are likely to cause dephasing between the excited state levels of the chromophores. In this case we would expect that the excitation will move incoherently between dimers at room temperature, recovering the hopping model. The question of localization of excitons including phonons in the theoretical description has been addressed in dimers by Friesner and Silbey[96] and in aggregates by Spano *et al.*[97] Clearly a detailed consideration of this problem in bacterial antennae will be required.

Recently, Xiao *et al.* have performed pump−probe experiments on membranes of *Rhodobacter capsulatus*, in which they find an anomalously large bleaching.[26] This result could be interpreted as a strong indication of exciton coupling over several pigments. Complications may arise from annihilation processes, and we feel that it is premature to conclude that excitation is delocalized from this result. Although the authors find that a doubling of the excitation energy does not lead to appreciable changes in the trapping kinetics, excitation densities must sometimes be varied over factors of 10 in order to discern the effects of annihilation (see Figure 5).

As a final comment, although we interpret our results on LH-1 within the framework of localized excitations, care should be taken when comparing to other systems. Minor changes in the energetics can change the picture drastically. In contrast with the LH-1 of *Rb. sphaeroides* studied here, in *Rps. viridis* the low-temperature LH-1 absorption and emission bands, as well as their polarization spectra, show structure[98] that may be hard to explain within the incoherent hopping model.

Summary

This work has directly revealed the extremely short time scale of excitation hopping within the LH-1 antenna complex of *Rb. sphaeroides*. We observe the process of fluorescence depolarization to occur on a time scale of $\sim$100 fs (dominant) and $\sim$400−500 fs. Using a ring structure derived from a recent electron diffraction map of LH-1 two-dimensional crystals,[17] we find that a Förster transfer model of incoherent hopping between BChl dimers can satisfactorily reproduce the depolarization time scale. The site-to-site hopping time is 80 fs. To account for the nonexponential anisotropy decay, we performed simulations which take into account the inhomogeneous distribution of donor and acceptor sites within the absorption band. We find that a model with an inhomogeneous distribution of width about equivalent to the homogeneous linewidth will reproduce the two-component depolarization for the M2192 membranes, whereas an inhomogeneity about twice the homogeneous linewidth is required for the much smaller isolated complexes ($N = 8$). Further, for the isolated complexes the separation between dimers and the hopping time appear to be much larger. Although structural evidence currently favors a symmetric ring structure, and there is certainly considerable evidence for an inhomogeneous antenna, our data cannot rule out an alternative model in which a clustering of pigments occurs (model B). This model can also account for the nonexponential depolarization behavior without requiring spectral inhomogeneity. Both models are consistent with the observed singlet−singlet annihilation time scale. We also have evidence for the persistence of vibrational wave packets in a 105 cm^{-1} mode of the excited state chromophore, for a time scale longer than the dominant phase of the hopping process. The frequency of these oscillations, which are absent in monomeric BChl *a*, supports the hypothesis that dimers comprise the LH-1 antenna. The persistence of the oscillations may result from coherence transfer in the energy-transfer process. However, once again, we cannot rule out the alternative explanation that the slow vibrational dephasing results from confinement produced by clusters of bacteriochlorophyll molecules.

Acknowledgment. We would like to thank S. N. Dikshit for preparing the detergent-isolated complexes. It is a pleasure to acknowledge several helpful discussions with David Oxtoby, Jeff Cina, Eric Hiller, Oscar Somsen, and Jan Leegwater. We thank Gerald Small for many useful comments on the manuscript. The work in Chicago was supported by the National Science Foundation and in Amsterdam by the Dutch Organization for Scientific Research (NWO) via the Foundation for Life Sciences (SLW). R.J. acknowledges the National Physical Science Consortium for a graduate fellowship.

References and Notes

(1) Van Grondelle, R.; Dekker, J. P.; Gillbro, T.; Sundström, V. *Biochim. Biophys. Acta* **1994**, *1187*, 1−65.
(2) Deisenhofer, J.; Epp, O.; Miki, K.; Huber, R.; Michel, H. *J. Mol. Biol.* **1984**, *180*, 385−398.
(3) Ermler, U.; Fritzsch, G.; Buchanan, S.; Michel, H. *Structure* **1994**, *2*, 925−936.
(4) Chang, C.-H.; Tiede, D.; Tang, J.; Smith, U.; Norris, J.; Schiffer, M. *FEBS Lett.* **1986**, *205*, 82−86.
(5) McDermot, J.; Prince, S.; Freer, A. A.; Hawthornethwaite-Lawless, A. M.; Papiz, M. Z.; Cogdell, R. J.; Isacs, N. W. *Nature* **1995**, *374*, 517−521.
(6) Zuber, H.; Brunisholz, R. A. In *Chlorophylls*; Scheer, H., Ed.; CRC Press: Boca Raton, FL, 1991; pp 627−719.
(7) Hunter, C. N.; Van Grondelle, R.; Olsen, J. D. *Trends Biochem. Sci.* **1989**, *14*, 72−76.
(8) Meckenstock, R. U.; Brunisholz, R. A.; Zuber, H. *FEBS Lett.* **1992**, *311*, 128−134. Meckenstock, R. U.; Krusche, K.; Brunisholz, R. A.; Zuber, H. *FEBS Lett.* **1992**, *311*, 135−138.
(9) Meckenstock, R. U.; Krusche, K.; Staehelin, L. A.; Cyrklaff, M.; Zuber, H. *Biol. Chem. Hoppe-Seyler* **1994**, *375*, 429−438.
(10) Francke, C.; Amesz, J. *Photosynth. Res.*, in press
(11) Kramer, H. J. M.; Pennoyer, J. D.; Van Grondelle, R.; Westerhuis, W. H. J.; Niederman, R. A.; Amesz, J. *Biochim. Biophys. Acta* **1984**, *767*, 335−344.
(12) Picorel, R.; L'Ecuyer, A.; Potier, M.; Gingras, G. *J. Biol. Chem.* **1986**, *261*, 3020−3024.
(13) Gingras, G.; Picorel, R. *Proc. Natl. Acad. Sci. U.S.A.* **1990**, *87*, 3405−3409.
(14) Van Mourik, F.; Van der Oord, C. J. R.; Visscher, K. J.; Parkes-Loach, P. S.; Loach, P. A.; Visschers, R. W.; Van Grondelle, R. *Biochim. Biophys. Acta* **1991**, *1059*, 111−119.
(15) Stark, W.; Kuhlbrandt, W.; Wildhaber, I.; Wehrli, E.; Muhlethaler, K. *EMBO J.* **1984**, *3*, 777−783.
(16) Boonstra, A. F.; Visschers, R. W.; Calkoen, F.; Van Grondelle, R.; Van Bruggen, E. F. J.; Boekema, E. J. *Biochim. Biophys. Acta* **1993**, *1142*, 181−188.
(17) Karrasch, S.; Bullough, P. A.; Ghosh, R. *EMBO J.* **1995**, *14*, 631−638.
(18) Chang, M. C.; Callahan, P. M.; Parkes-Loach, P. S.; Cotton, T. M.; Loach, P. A. *Biochemistry* **1990**, *29*, 421−429.
(19) Miller, J. F.; Hinchigeri, S. B.; Parkes-Loach, P. S.; Callahan, P. M.; Sprinkle, J. R.; Riccobono, J. R.; Loach, P. A. *Biochemistry* **1987**, *26*, 5055−5062.
(20) Parkes-Loach, P. S.; Sprinkle, J. R.; Loach, P. A. *Biochemistry* **1988**, *27*, 2718−2727.
(21) Visschers, R. W.; Chang, M. C.; Van Mourik, F.; Parkes-Loach, P. S.; Heller, B. A.; Loach, P. A.; Van Grondelle, R. *Biochemistry* **1991**, *30*, 5734−5742.
(22) Van Mourik, F.; Visscher, K. J.; Mulder, J. M.; Van Grondelle, R. *Photochem. Photobiol.* **1993**, *57*, 19−23.
(23) Visser, H. M.; Somsen, O. J. G.; Van Mourik, F.; Lin, S.; Van Stokkum, I.; Van Grondelle, R. *Biophys. J.* **1995**, *69*, 1083−1099.

(24) Van Mourik, F.; Corten, E.; Van Stokkum, I. H. M.; Visschers, R. W.; Loach, P. A.; Kraayenhof, R.; Van Grondelle, R. In *Research in Photosynthesis;* Murata, N., Ed.; Kluwer Academic Publishers: Dordrecht, The Netherlands, 1992; Vol. 1, pp 101−104.
(25) Reddy, N. R. S.; Small, G. J. *J. Chem. Phys.* **1991**, *94*, 7545−7546. Reddy, N. R. S.; Picorel, R.; Small, G. J. *J. Phys. Chem.* **1992**, *96*, 6458−6464.
(26) Xiao, W.; Lin, S.; Taguchi, A. K. W.; Woodbury, N. W. *Biochemistry* **1994**, *33*, 8313−8322.
(27) Boonstra, A. F.; Germeroth, L.; Boekema, E. *Biochim. Biophys. Acta* **1994**, *1184*, 227−234.
(28) Hunter, C. N.; Van Grondelle, R.; Van Dorssen, R. J. *Biochim. Biophys. Acta* **1989**, *973*, 383−389.
(29) Bergstrom, H.; Sundström, V.; Van Grondelle, R.; Åkesson, E.; Gillbro, T. *Biochim. Biophys. Acta* **1986**, *852*, 279−287.
(30) Van Grondelle, R.; Bergstrom, H.; Sundström, V.; Gillbro, T. *Biochim. Biophys. Acta* **1987**, *894*, 313−326.
(31) Bergstrom, H.; Sundström, V.; Van Grondelle, R.; Gillbro, T.; Cogdell, R. J. *Biochim. Biophys. Acta* **1988**, *936*, 90−98.
(32) Bergström, H.; Westerhuis, W. H. J.; Sundström, V.; Van Grondelle, R.; Niederman, R. A.; Gillbro, T. *FEBS Lett.* **1988**, *233*, 12−16.
(33) Sundström, V.; Van Grondelle, R.; Bergström, H.; Åkesson, E.; Gillbro, T. *Biochim. Biophys. Acta* **1986**, *851*, 431−446.
(34) Beekman, L. M. P.; Van Mourik, F.; Jones, M. R.; Visser, H. M.; Hunter, C. N.; Van Grondelle, R. *Biochemistry* **1994**, *33*, 3143−3147.
(35) Timpmann K.; Freiberg, A.; Godik, V. I. *Chem. Phys. Lett.* **1991**, *182*, 617−622.
(36) Freiberg, A.; Timpmann, K. *J. Photochem. Photobiol. B: Biol.* **1992**, *15*, 151−158.
(37) Freiberg, A.; Godik, V. I.; Pullerits, T.; Timpmann, K. *Biochim. Biophys. Acta* **1989**, *973*, 93−104.
(38) Den Hollander, W. Th. F.; Bakker, J. G. C.; Van Grondelle, R. *Biochim. Biophys. Acta* **1983**, *725*, 492−507.
(39) Bakker, J. G. C.; Van Grondelle, R.; Den Hollander, W. Th. F. *Biochim. Biophys. Acta* **1983**, *725*, 508−518.
(40) Valkunas, L.; Liuolia, V.; Freiberg, A. *Photosynth. Res.* **1991**, *27*, 83−95.
(41) Raja, N.; Reddy, S.; Lyle, P. A.; Small, G. J. *Photosynth. Res.* **1992**, *31*, 167−194.
(42) De Caro, C.; Visschers, R. W.; Van Grondelle, R.; Volker, S. *J. Luminescence* **1994**, *58*, 149−153.
(43) Visschers, R. W.; Van Mourik, F.; Monshouwer, R.; Van Grondelle, R. *Biochim. Biophys. Acta* **1993**, *1141*, 238−244.
(44) Van Mourik, F.; Visschers, R. W.; Van Grondelle, R. *Chem. Phys. Lett.* **1992**, *193*, 1−7.
(45) Pullerits, T.; Visschers, K. J.; Hess, S.; Sundström, V.; Freiberg, A.; Timpmann, K.; Van Grondelle, R. *Biophys. J.* **1994**, *66*, 236−248.
(46) Pullerits, T.; Freiberg, A. *Biophys. J.* **1992**, *63*, 879−896.
(47) Pullerits, T.; Van Mourik, F.; Monshouwer, R.; Visschers, R. W.; Van Grondelle, R. *J. Luminescence* **1994**, *58*, 168−171.
(48) Leupold, D.; Voigt, B.; Pfeiffer, M.; Bandilla, M.; Scheer, H. *Photochem. Photobiol.* **1993**, *57*, 24−28.
(49) Pullerits, T.; Chachisvilis, M.; Jones, M. R.; Hunter, C. N.; Sundström, V. *Chem. Phys. Lett.* **1994**, *224*, 355−365.
(50) Chachisvilis, M.; Pullerits, T.; Jones, M. R.; Hunter, C. N.; Sundström, V. *Chem. Phys. Lett.* **1994**, *224*, 345−351.
(51) Vos, H. V.; Jones, M. R.; Hunter, C. N.; Breton, J.; Lambry, J.-C.; Martin, J.-L. *Biochemistry* **1994**, *33*, 6750−6757.
(52) Stanley, R. J.; Boxer, S. G. *J. Phys. Chem.* **1995**, *99*, 859−863.
(53) Xie, X.; Du, M.; Mets, L.; Fleming, G. R. *Proceedings of the International Society of Optical Engineers,* OE/LASE, SPIE: Bellingham, WA, 1992; p 1640. Rosenthal, S. J.; Jimenez, R.; Fleming, G. R.; Kumar, P. V.; Maroncelli, M. *J. Mol. Liquids* **1994**, *60*, 25−56.
(54) Paillotin, G.; Geacintov, N. E.; Breton, J. *Biophys. J.* **1983**, *44*, 65−77.
(55) Van Grondelle, R. *Biochim. Biophys. Acta* **1985**, *811*, 147−195.
(56) Monger, T. G.; Parson, W. W. *Biochim. Biophys. Acta* **1977**, *460*, 393−407.
(57) Cross, A. J.; Fleming, G. R. *Biophys. J.* **1984**, *46*, 45−56.
(58) Van Dorssen, R. J.; Hunter, C. N.; Van Grondelle, R.; Korenhof, A. H.; Amesz, J. *Biochim. Biophys. Acta* **1988**, *932*, 179−188.
(59) In principle, S−S annihilation poses a problem for the deconvolution of the fast phases in the signal. Since annihilation is a nonlinear effect, fitting procedures which convolute a set of lifetimes with the instrument response function are no longer adequate. The annihilation processes depend on the true pulse shape, which is generally unknown.
(60) Monger, T. G.; Cogdell, R. J.; Parson, W. W. *Biochim. Biophys. Acta* **1976**, *449*, 136−153.
(61) Vos, M.; Van Grondelle, R.; Van dr Kooij, F. W.; Van der Poll, D.; Amesz, J.; Duysens, L. N. M. *Biochim. Biophys. Acta* **1986**, *850*, 501−512.
(62) Deinum, G.; Aartsma, T. J.; Van Grondelle, R.; Amesz, J. *Biochim. Biophys. Acta* **1989**, *976*, 63−69.
(63) Joo, T.-H.; Jia, Y.; Yu, J.; Jonas, D.; Fleming, G. R. *J. Phys. Chem.,* submitted.
(64) Jean, J.; Chan, C.-K.; Fleming, G. R. *Isr. J. Chem.* **1988**, *28*, 169−175.
(65) Somsen, O. J. G.; Van Mourik, F.; Van Grondelle, R.; Valkunas, L. *Biophys. J.* **1994**, *66*, 1580−1596.
(66) Magde, D. *J. Chem. Phys.* **1978**, *68*, 3717−3733.
(67) This assumes a monomer BChl *a* Q_y transition dipole strength of 41 D^2 and an angle between monomer Q_y transition moments of 30°. See ref 64 and references therein.
(68) Jimenez, R.; Dikshit, S. N.; Fleming, G. R. Unpublished data.
(69) Bradforth, S. E.; Jimenez, R.; Fleming, G. R. Manuscript in preparation.
(70) Pearlstein, R. M. *Photochem. Photobiol.* **1982**, *35*, 835−844.
(71) Van Kampen, N. G. *Stochastic processes in physics and chemistry*; North Holland Physics: Amsterdam, The Netherlands, 1981. Leegwater, J. A. Personal communication.
(72) The effect of inhomogeneity on the migration time is rather complex. The simulations performed to reproduce the effect of inhomogeneity on the anisotropy decay indicate that the average hopping time is slowed down by about a factor of 2 for 500 cm^{-1} antenna inhomogeneity. However, as the equilibration process mainly consists of downhill energy transfer processes, the migration term may be less strongly influenced than this average hopping rate. For large systems the presence of bottlenecks may somewhat modify this simplification: see for example ref 45.
(73) Juzeliunas, G. *Chem. Phys.* **1991**, *151*, 169−178.
(74) Savikhin, S.; Struve, W. S. *Biophys. J.* **1994**, *67*, 2002−2007.
(75) Johnson, S. G.; Tang, D.; Jankowiak, R.; Hayes, J. M.; Small, G. J.; Tiede, D. M. *J. Phys. Chem.* **1989**, *93*, 5953−5957.
(76) Cherepy, N. J.; Shreve, A. P.; Moore, L. J.; Franzen, S.; Boxer, S. G.; Mathies, R. A. *J. Phys. Chem.* **1994**, *98*, 6023−6029.
(77) Jimenez, R. J.; Dikshit, S. N.; Bradforth, S. E.; Fleming, G. R. In preparation.
(78) Vos, M. H.; Jones, M. R.; McGlynn, P.; Hunter, C. N.; Breton, J.; Martin, J.-L. *Biochim. Biophys. Acta* **1994**, *1186*, 117−122.
(79) Vos, H. M.; Rappaport, F.; Lambry, J.-C.; Breton, J.; Martin, J.-L. *Nature*, **1993**, *363*, 320−325.
(80) Wang, Q.; Schoenlein, R. W.; Peteanu, L. A.; Mathies, R. A.; Shank, C. V. *Science* **1994**, *266*, 422−424.
(81) Scherer, N. F.; Jonas, D. M.; Fleming, G. R. *J. Chem. Phys.* **1993**, *99*, 153−168.
(82) Zadoyan, R.; Li, Z.; Masters, C. C.; Apkarian, V. A. *J. Chem. Phys.* **1994**, *101*, 6648−6657.
(83) Jean, J. M.; Fleming, G. R. *J. Chem. Phys.,* accepted.
(84) Knox, R. S.; Gulen, D. *Photochem. Photobiol.* **1993**, *57*, 40−43.
(85) Wynne, K.; Hochstrasser, R. M. *Chem. Phys.* **1993**, *171*, 179−188.
(86) Matro, A.; Cina, J. A. *J. Phys. Chem.* **1995**, *99*, 2568.
(87) Du, M.; Xie, X. L.; Mets, L.; Fleming, G. R. *J. Phys. Chem.* **1994**, *98*, 4736−4741.
(88) Cogdell, R. J. Private communication.
(89) Scholes, G. D.; Ghiggino, K. P. *J. Phys. Chem.* **1994**, *98*, 4580−4590.
(90) Thompson, M. A.; Schenter, G. K. *J. Phys. Chem.* **1995**, *99*, 6374−6386.
(91) Gottfried, D. S.; Stocker, J. W.; Boxer, S. G. *Biochim. Biophys. Acta* **1991**, *1059*, 63−75.
(92) Moser, C. C.; Keske, J. M.; Warncke, K.; Farid, R. S.; Dutton, P. L. *Nature* **1992**, *355*, 796−802.
(93) Fidder, H.; Knoester, J.; Wiersma, D. A. *J. Chem. Phys.* **1991**, *95*, 7880−7890.
(94) Dracheva, T. V.; Noroderezhkin, V. I.; Razjivin, A. P. *Chem. Phys.* **1995**, *194*, 223−235.
(95) Loppnow, G. R.; Mathies, R. A.; Middnedorf, T. R.; Gottfried, D. S.; Boxer, S. G. *J. Phys. Chem.* **1992**, *96*, 737−745.
(96) Friesner, R. A.; Silbey, R. *J. Chem. Phys.* **1981**, *75*, 3925−3936.
(97) Spano, F. C.; Kuklinski, J. R.; Mukamel, S. *Phys. Rev. Lett.* **1990**, *65*, 211−214.
(98) Monshouwer, R. M.; Visschers, R. W.; Van Mourik, F.; Freiberg, A.; Van Grondelle, R. *Biochim. Biophys. Acta* **1995**, *1229*, 373−380.

JP9515038